Thermodynamics of the ligandin function of human class Alpha glutathione transferase A1-1: energetics of organic anion ligand binding

Yasien SAYED*, Judith A. T. HORNBY*, Marimar LOPEZ† and Heini DIRR*[1]

*Protein Structure-Function Research Programme, School of Molecular and Cell Biology, University of the Witwatersrand, Johannesburg 2050, South Africa, and †Department of Biochemistry and Molecular Biology, Pennsylvania State University College of Medicine, Hershey, PA 17033-0850, U.S.A.

In addition to their catalytic functions, cytosolic glutathione S-transferases (GSTs) are a major reserve of high-capacity binding proteins for a large variety of physiological and exogenous non-substrate compounds. This ligandin function has implicated GSTs in numerous ligand-uptake, -transport and -storage processes. The binding of non-substrate ligands to GSTs can inhibit catalysis. In the present study, the energetics of the binding of the non-substrate ligand 8-anilino-1-naphthalene sulphonate (ANS) to wild-type human class Alpha GST with two type-1 subunits (hGSTA1-1) and its ΔPhe-222 deletion mutant were studied by isothermal titration calorimetry. The stoichiometry of binding to both proteins is one ANS molecule per GST subunit with a greater affinity for the wild-type ($K_d = 65\ \mu M$) than for the ΔPhe-222 mutant ($K_d = 105\ \mu M$). ANS binding to the wild-type protein is enthalpically driven and it is characterized by a large negative heat-capacity change, ΔC_p. The negative ΔC_p value for ANS binding indicates a specific interface with a significant hydrophobic component in the protein–ligand complex. The negatively charged sulphonate group of the anionic ligand is apparently not a major determinant of its binding. Phe-222 contributes to the binding affinity for ANS and the hydrophobicity of the binding site.

Key words: ANS, isothermal titration calorimetry.

INTRODUCTION

The cytosolic glutathione S-transferases (GSTs; EC 2.5.1.18) are a supergene family of phase II enzymes that detoxify endogenous and exogenous substances by conjugating them to GSH. As a consequence of their catalytic function, GSTs have been implicated in the development of resistance of tumours towards various alkylating, electrophilic anti-canccer drugs [1–4]. Furthermore, because of their abundance and binding properties, they represent a large reserve of high-capacity binding proteins that can sequester a large variety of structurally diverse non-substrate ligands with high-to-moderate affinity [5]. This ligand-binding (ligandin) function has implicated GSTs in the intracellular uptake and transport of hydrophobic non-substrate compounds. They may also serve to prevent the accumulation of hydrophobic molecules at lipophilic sites within the cell. The ligandin function has implications for the catalytic function of GSTs in that ligand binding can inhibit catalysis.

Unlike the catalytic properties of GSTs, which have been studied extensively [6], very little is known about the structural and thermodynamic basis of their ligandin function. Although much data is available regarding the ligands involved, their affinities for various GSTs, and the impact of non-substrate ligand binding on catalytic function, details regarding the location and properties of ligand-binding sites are not clear. Furthermore, since indirect methods (e.g. fluorescence spectroscopy) have been used to determine the binding stoichiometry for many of the ligands, there is uncertainty concerning the number of sites involved. When the first GST structure was solved, we proposed that the cleft located along the dimer interface might serve to bind non-substrate ligands [7,8]. Subsequently, the cleft was shown by crystallography to be the binding site for the drug praziquantel in schistosomal GST [9] and for a glutathione conjugate in class Sigma GST with two type-1 subunits [10]. Fluorescence resonance energy transfer and affinity-labelling studies have also implicated the cleft in binding 8-anilino-1-naphthalene sulphonate (ANS) and aflatoxin B_1 [11,12], and steroid sulphates [13]. The dimeric structure of GSTs is therefore not only important for stabilizing the tertiary structures of GST subunits [14], it is also a requirement for the formation of non-substrate binding sites at the dimer interface.

Another ligandin site for non-substrate ligands was identified at the hydrophobic region of both active sites in the crystal structures of human class Pi GST with two type-1 subunits [15]. Interestingly, these crystal structures have also indicated the presence of a potential non-substrate binding site between α1, β2 and α8 in each subunit, to which sulphonate buffer anions bind [15–18]. This hydrophobic site is not related to the active site but may be involved in non-competitive inhibition of the enzyme via a ligand-induced conformational change in helix 8, the C-terminus of which is close to the active site. This ligandin site might be involved in binding bromosulphophthalein [12,17,19,20], bilirubin [21], fatty acids [22] and 2-hydroxy-5-nitrobenzyl alcohol [23]. The stoichiometry of ligand binding to dimeric GSTs appears to depend on the size of the ligand and on whether it binds the intersubunit cleft (1:1 or 2:1) or the buffer binding site (2:1). Stoichiometry of organic anion binding has also been shown to be dependent on the subunit type; i.e. high-affinity binding occurs on the Alpha 1 but not the Alpha 2 subunit, resulting in stoichiometry ratios of 2:1 for Alpha 1–1 homodimers and 1:1 for Alpha 1–2 heterodimers [24,25].

In the present study, the energetics of the binding of the non-substrate organic anion ANS to human class Alpha GST with two type-1 subunits (hGSTA1-1) was determined by isothermal titration calorimetry (ITC). Unlike GSTs from other gene classes, class Alpha GSTs have an extended C-terminal region [26,27]

Abbreviations used: A-LBP, adipose lipid-binding protein; ANS, 8-anilino-1-naphthalene sulphonate; ASA, solvent-accessible surface area; GST, glutathione S-transferase; hGSTA1-1, human class Alpha GST with two type-1 subunits; ΔPhe-222, deletion of Phe-222 from the C-terminus of hGSTA1-1; I-FABP, intestinal fatty acid-binding protein; ITC, isothermal titration calorimetry; ΔC_p, heat-capacity change.

[1] To whom correspondence should be addressed (e-mail 089dirr@cosmos.wits.ac.za).

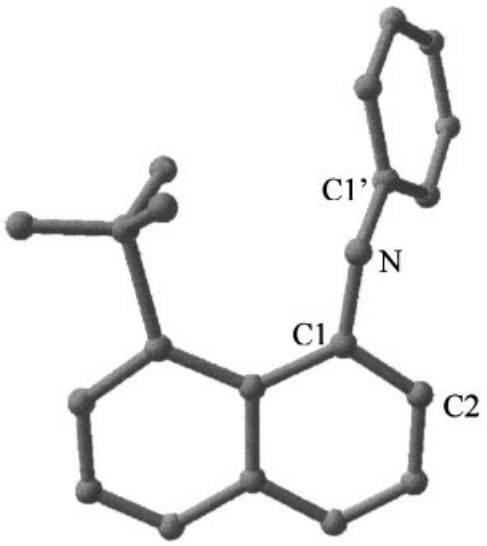

Figure 1 The structure of ANS

The conformational flexibility of ANS is described by two dihedral angles. Rotation occurs about the N–C1′ bond as well as the angle defined by C1′–N–C1–C2 from the anilino and naphthyl rings.

that is implicated in ligandin function [28]. The role of the ultimate residue Phe-222, located near the cleft at the dimer interface, in ligandin function was also addressed. Although we have no structural detail for the complex between hGSTA1-1 and ANS, a calorimetric analysis of its binding properties should provide useful information about the thermodynamics for the molecular recognition process for ligands. ANS, which is an amphipathic anion due to its negatively charged sulphonate and hydrophobic moieties (Figure 1), is widely used as a fluorescent probe to monitor structured hydrophobic surface areas during the folding/unfolding of proteins, including GSTs ([29] and references therein).

EXPERIMENTAL

Materials

The wild-type hGSTA1-1 protein was overexpressed using the plasmid pKHA1 (a gift from Professor B. Mannervik, Uppsala University, Uppsala, Sweden) transformed into *Escherichia coli* BL21 cells containing the pLysS plasmid. The protein was purified from a *S*-hexylglutathione affinity column as described previously [27,30]. The purity of the protein was confirmed by SDS/PAGE [31] and size-exclusion chromatography/HPLC. The dimeric protein concentration was calculated spectrophotometrically using a molar absorption coefficient (ϵ) of 38 200 $M^{-1} \cdot cm^{-1}$ at 280 nm [28]. ANS was purchased from Sigma and its concentration in solution was determined spectrophotometrically at 350 nm using $\epsilon = 4950\ M^{-1} \cdot cm^{-1}$.

The ΔPhe-222 mutant (with Phe-222 deleted from the C-terminus of hGSTA1-1) was generated using the pKHA1 plasmid. The following primers were used to generate the deletion mutant using the ExSite mutagenesis kit from Stratagene: F222 STOP FWD, 5′-GGAAGATCTTCAGG**TAA**TAATAACGC-AGTCATGG-3′, and F222 STOP REV, 5′-TTGCTTCTTCTA-AAGATTTCTCATCCATGGG-3′. The underlined nucleotide sequence represents the translationally silent mutation that encodes for the diagnostic *Bgl*II restriction site. The codon shown in bold letters represents the Phe-222 codon that has been replaced by a stop codon, thus generating the ΔPhe-222 deletion mutant. The cDNA region was sequenced using an ABI Prism 310 genetic analyser from PE Applied Biosystems to confirm the deletion of Phe-222 from the C-terminus and to verify the absence of any unwanted mutations. The mutant was purified under the same conditions as described above for the wild-type protein.

Enzyme activity studies

S-Conjugating activity with 1-chloro-2,4-dinitrobenzene and GSH was measured spectrophotometrically at 340 nm ($\epsilon = 9600\ M^{-1} \cdot cm^{-1}$) [32]. Peroxidase activity was determined with cumene hydroperoxide as a substrate as described previously [33]. All enzymic rates were corrected for the corresponding non-enzymic rates.

Fluorescence studies

Fluorescence emission spectra were measured in a Hitachi model 850 spectrofluorimeter. Proteins were excited at 295 nm, to obtain tryptophan fluorescence spectra. The binding of ANS to protein was monitored using enhanced fluorescence of the dye when excited at 390 nm [28].

Equilibrium unfolding studies

Reversibility and equilibrium unfolding studies with urea as a denaturant were performed as described previously [34]. Protein concentration was 1 μM and the concentration of urea ranged from 0 to 8 M. Structural changes were monitored by tryptophan fluorescence. Analysis of the unfolding transition to obtain the unfolding parameters $\Delta G(H_2O)$ (the change in free energy of unfolding in the absence of denaturant) and m value (the dependence of ΔG on denaturant concentration) was performed as previously described [35].

ITC

ITC enables determination of thermodynamic parameters [enthalpy change (ΔH), ΔG and entropy change (ΔS)], dissociation constant (K_d) and stoichiometry (N) of binding by direct measurement of the released or absorbed heat. Titration experiments were preformed using the VP-ITC calorimeter from MicroCal (Northampton, MA, U.S.A.) as described previously [36,37]. Protein was dialysed (3500 Da molecular-mass cut-off) exhaustively against 20 mM sodium phosphate buffer, pH 6.5, and the stock solution of ANS (3.6 mM) was prepared in the final dialysate buffer. Phosphate has a very low enthalpy of ionization (3.77–5.12 kJ/mol) [38,39], so the binding enthalpies reported for the interaction between ligand and protein do not reflect any contribution due to buffer protonation. Titrations were performed by injecting 3 μl of ANS stock into the ITC sample cell containing 0.06 mM protein subunit. Heats of dilution were determined by titrating ligand into buffer and the total observed heats of binding were corrected for heats of dilution prior to data analysis. Concentrations of protein and ANS were verified spectrophotometrically and effects due to light scattering were corrected [40] before data fitting. Raw data were integrated and processed with the ORIGIN 5 analysis software (MicroCal). The independent variables for non-linear least-squares fitting of titration curves with ORIGIN 5 are K_d, ΔH and N. Once K_d and ΔH were obtained, the free energy and entropy of binding were calculated using the following equations: $\Delta G = -RT \ln(1/K_d)$ and $\Delta G = \Delta H - T\Delta S$, where T is the absolute temperature in K.

RESULTS

The deletion of Phe-222 from the C-terminus of hGSTA1-1 did not impact on the protein's structural or catalytic properties, or its stability. Secondary, tertiary and quaternary structures remained unchanged as shown by far-UV CD, fluorescence and size-exclusion HPLC respectively (results not shown). Unfolding of ΔPhe-222 with urea was reversible (recoveries in excess of 95%) and its stability parameters [$\Delta G(H_2O)$ and m value] were similar to those reported for the wild-type protein [34]. The specific activities with 1-chloro-2,4-dinitrobenzene were 52 ± 2 and 54 ± 3 μmol/min per mg for wild-type and ΔPhe-222 respectively. For cumene hydroperoxide they were 9.4 ± 0.2 and 10.6 ± 0.2 μmol/min per mg respectively. ΔPhe-222 did, however, display reduced ANS binding, as shown by the fluorescence spectra in Figure 2. Furthermore, the emission maximum for ANS bound to ΔPhe-222 was 480 nm, compared with 475 nm for ANS bound to wild-type hGSTA1-1.

The raw and normalized integrated titration data shown in Figure 3 are representative of the exothermic binding of the ANS anion to wild-type and ΔPhe-222 mutant hGSTA1-1. For both proteins, the integrated data for ANS binding fit well to a model based on one independent binding site per subunit. The calorimetrically determined binding affinity for ANS to the wild-type protein (65 μM) agrees with that obtained from fluorescence studies (55 μM) [41]. Deletion of Phe-222 from the C-terminus of hGSTA1-1 reduced the affinity for ANS by approx. 2-fold (105 μM), in agreement with the fluorescence data shown below. The enthalpy and entropy of binding of ANS to hGSTA1-1 were temperature-dependent but, because they compensate each other, ΔG was relatively insensitive to temperature (Figure 4). ANS binding to wild-type hGSTA1-1 was driven enthalpically and below 17 °C entropy made a positive contribution towards binding. Although binding was entropically opposed above 17 °C this effect was compensated for by a large enthalpy of binding at these temperatures. ANS binding to the mutant protein was driven enthalpically at temperatures below 50 °C. Entropy contributes favourably towards binding at temperatures above 10 °C. The linear temperature dependence of ΔH indicates that the heat-capacity change (ΔC_p) for ANS binding to both proteins was independent of temperature within the experimental temperature range. The magnitude of ΔC_p for ANS binding to wild-type hGSTA1-1 was -0.84 ± 0.13 kJ/mol per K and for binding to ΔPhe-222 it was $+0.53 \pm 0.05$ kJ/mol per K.

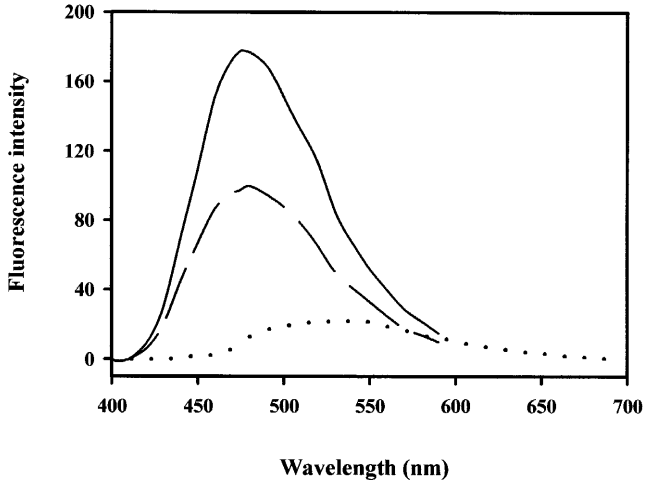

Figure 2 Emission spectra of ANS binding to wild-type and ΔPhe-222 hGSTA1-1

ANS (100 μM) was added to 1 μM wild-type and ΔPhe-222 protein. ANS was excited selectively at 390 nm, and the wavelength emission spectra were monitored. The spectra of ANS binding to wild-type and ΔPhe-222 proteins are represented by solid and dashed lines respectively. These spectra were corrected for the contribution of free unbound ANS in buffer (dotted line).

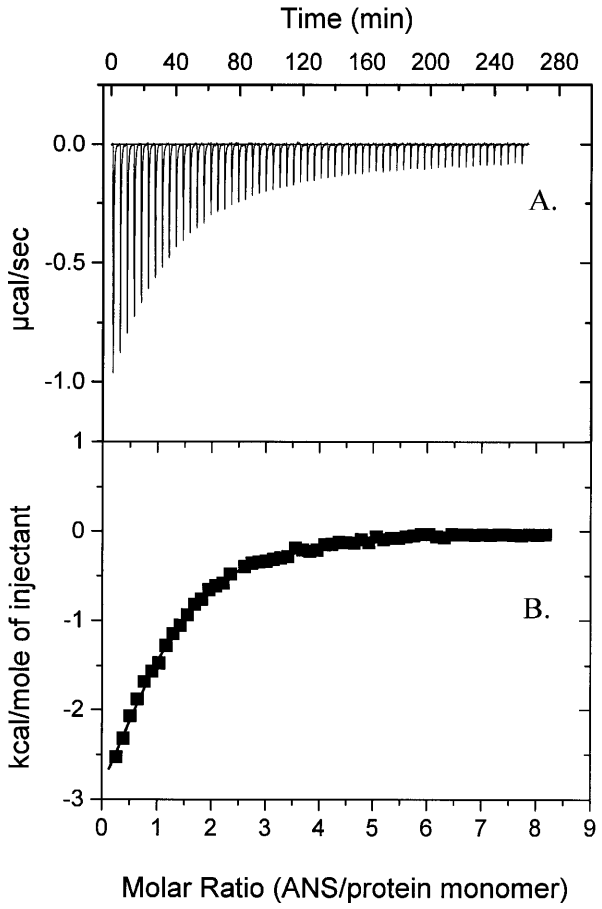

Figure 3 Representative calorimetric titration profile of the binding of the organic anionic dye ANS to wild-type hGSTA1-1 protein

The experiment was performed at 10 °C. The conditions were: 0.06 mM protein monomer and 3.6 mM ANS in 20 mM sodium phosphate buffer, pH 6.5, containing 0.1 M NaCl, 1 mM EDTA and 0.02% sodium azide. (**A**) Exothermic heat effects associated with the injection of ANS into the ITC sample cell containing the wild-type protein. (**B**) Binding isotherm (corrected for heats of dilution) corresponding to the data in (**A**). The solid line through the data represents the line of best fit obtained using ORIGIN 5 software.

DISCUSSION

ANS binding site and stoichiometry

The stoichiometry of ANS binding to wild-type and ΔPhe-222 hGSTA1-1, as determined by ITC, is one ANS molecule/protein subunit (i.e. two ANS molecules/dimer). Although the exact location of the ANS binding site in the hGSTA1 subunit is unknown, a fluorescence resonance energy-transfer study indicated binding of ANS at the V-shaped cleft along the dimer interface [11]. The C-terminus of helix 9, also located near

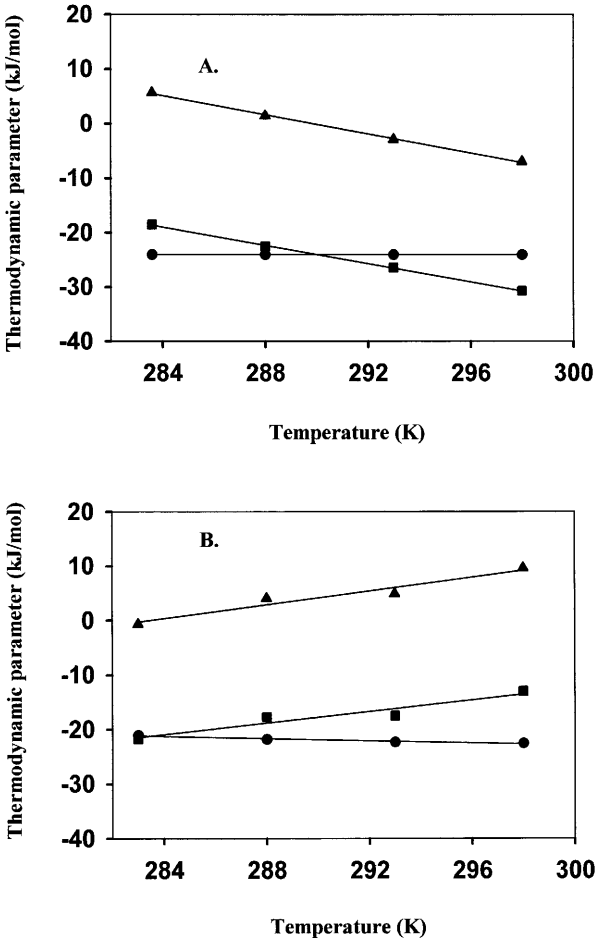

Figure 4 Thermodynamic parameters for the binding of ANS to the wild-type (A) and ΔPhe-222 (B) hGSTA1-1 proteins

Symbols: ●, ■ and ▲ represent ΔG, ΔH and $T\Delta S$ values, respectively, which were obtained at different temperatures. The solid lines represent linear regressions.

the dimer interface, is adjacent to the ANS site and modulates ANS binding [28]. Other non-substrate ligands that bind the V-shaped cleft include aflatoxin B_1 [12], oestradiol disulphate [13] and 5-{[2-[(acetyl)amino]ethyl]amino}-naphthalene-1-sulphonic acid (AEDANS) [42]. The stoichiometry of binding apparently varies according to the size of the ligand. Large ligands, such as oestradiol disulphate, bind with a stoichiometry of one ligand/dimer [13]. Binding at one site sterically prevents binding to the other symmetry-related site at the dimer interface. Ligand–ligand steric effects at the dimer interface cleft also explain the 1:1 binding stoichiometry for the anti-schistosomal drug praziquantel bound to a schistosomal GST [9], and a GSH S-conjugate bound to class Sigma GST 1-1 [10]. Binding of ANS to GSTs is not accompanied by any major protein conformational change ([20,42], and R. Ohlmeyer, W.H. Kaplan and H. Dirr, unpublished work).

Energetics of ANS binding

Phe-222 does not play an important role in regulating the dynamics of the C-terminus, as the catalytic function of the ΔPhe-222 mutant was comparable with that of the wild-type enzyme. Phe-222, however, does contribute towards the binding of ANS to hGSTA1-1, as its deletion results in diminished affinity for the dye. The majority of energy for the binding of the ANS anion to wild-type and ΔPhe-222 hGSTA1-1 derives from exothermic enthalpic effects. The binding of ANS to various proteins and cationic polyamino acids has also been shown to be enthalpically driven [43–45]. For wild-type hGSTA1-1, entropy contributes favourably below approx. 17 °C, whereas it opposes binding above this temperature. Binding of ANS to lipid-binding proteins (stoichiometry of one ANS/protein) was also found to be enthalpically driven with entropy making a positive contribution towards binding below approx. 14 °C for intestinal fatty acid-binding protein (I-FABP) [43] and approx. 25 °C for adipose lipid-binding protein (A-LBP) [44]. Above the temperature where the sign of entropy changes, the unfavourable entropy is compensated for by the large binding enthalpies for the three ANS-binding proteins. For ΔPhe-222 hGSTA1-1, entropy contributes favourably towards ANS binding above 10 °C.

ANS binding to wild-type hGSTA1-1 is characterized by a negative change in heat capacity (-0.84 ± 0.13 kJ/mol per K). ΔC_p values of similar magnitude were obtained for the binding of ANS to I-FABP (-1.18 kJ/mol per K) [43] and A-LBP (-0.922 kJ/mol per K) [44]. The linearity in the ΔC_p determination for wild-type and ΔPhe-222 proteins excludes the possibility of thermal effects on the structure of hGSTA1-1. In particular, the C-terminus of the protein, which is involved in ligandin function, is unstable and unfolds at low denaturant concentrations [28]. Formation of a bimolecular interface between protein and ligand results in the removal of groups from solvent (and thus dehydration of their surfaces), and the packing of these groups within the protein. A negative ΔC_p can be expected for the reduction of solvent access to non-polar surfaces [46]. Furthermore, a relatively large negative ΔC_p is indicative of a specific interface in the protein–ligand complex [47]. Non-specific binding events often exhibit very little temperature-dependence on enthalpy [48]. The negative ΔC_p, therefore, suggests the presence of a significant hydrophobic component in the hGSTA1-1–ANS interaction. This is supported by the significant increase in ΔC_p upon deletion of Phe-222.

The ΔC_p upon binding can be reasonably well predicted from the changes in the solvent-accessible surface area (ASA) upon complex formation [37,49–51]. This requires knowledge of the three-dimensional structure. However, the crystal structure for hGSTA1-1 in complex with ANS has not been solved. On the other hand, a crystal structure of Sj26GST (the 26 kDa GST from *Schistosoma japonicum*) in complex with the drug praziquantel is known [9]. We have used this crystal structure as a first approximation for the ANS binding because both ligands are similar in size and, when free in solution, have comparable ASA values. For our calculations we have used the Protein Data Bank access code 1GTB for the ligand praziquantel bound to the protein. The surface area for the free protein was calculated based on the complex after removing the co-ordinates for the ligand. In this way, possible structural changes upon ligand binding are not taken into account. Moreover, there is experimental evidence that no major conformational change occurs upon ANS binding to GST [42]. The change in ASA upon complex formation, ΔASA, was estimated as:

$$\Delta ASA = ASA_{dimer-praziquantel} - ASA_{dimer} - ASA_{praziquantel} \quad (1)$$

where $ASA_{dimer-praziquantel}$ is the ASA of the complex, ASA_{dimer} is the ASA for the protein in the absence of ligand and $ASA_{praziquantel}$ is the ASA for the ligand. The ASA values were calculated using the NACCESS computer program [designed by S.J. Hubbard and J.M. Thornton (1993), Department of Biochemistry and

Molecular Biology, University College London, London, U.K.]. The ΔASA values were used to calculate the expected ΔC_p upon complex formation as [37,51]:

$$\Delta C_p = 2.14 \cdot \Delta ASA_{alp} + 1.55 \cdot \Delta ASA_{arm} - 1.81 \cdot \Delta ASA_{bb} - 0.88 \cdot \Delta ASA_{pol} \quad (2)$$

where the subscripts alp, arm, bb and pol represent the changes in ASA for aliphatic, aromatic, backbone and polar atoms respectively. The numerical coefficients are expressed in J/(K·mol·Å²). For our calculations we have considered only the changes in ASA for aliphatic and aromatic residues because the polar atoms of the ligand remain solvent-exposed and no significant changes in the ΔASA_{pol} and ΔASA_{bb} values of the protein were observed. Based on the ΔASA_{arm} and ΔASA_{alp} values calculated according to eqn (2), the expected ΔC_p, calculated according to eqn (2), is -1.0 kJ/mol per K. This value correlates well with the experimental one (-0.84 ± 0.13 kJ/mol per K). Even though the structural calculations were done for a different ligand, they provide further support for the importance of hydrophobic interactions in the binding. Hydrophobic interactions also play a key role in determining the stability of ANS complexes with A-LBP [44] and I-FABP [43]. Apparently, there are no significant ionic interactions between the negatively charged sulphonate group of ANS and protein. This is contrary to the findings of Matulis and Lovrien [45] that the binding of ANS to proteins is primarily dependent on ion-pair formation where the sulphonate group is the major binding determinant and the anilinonaphthalene moiety of ANS only reinforces the binding.

The ANS site in hGSTA1-1 is not strictly hydrophobic, as indicated by the fluorescence emission maximum of 475 nm for ANS bound to wild-type hGSTA1-1. This is compared with the emission maximum of 545 nm for ANS in water and of 454 nm for ANS bound to the highly hydrophobic site in apomyoglobin [52]. The polarity of the ANS site in hGSTA1-1 appears to be similar to the surface site in chymotrypsin [53], and the cavity sites in I-FABP [43] and A-LBP [44], and, like these sites, the hGSTA1-1 site is apparently not anhydrous. The polarity of the ANS site in hGSTA1-1 is increased by the deletion of Phe-222. Because ANS fluorescence is quenched by water, the fluorescence intensity of protein-bound ANS is highly dependent upon its accessibility to water [43,45]. The fluorescence enhancement of ANS bound to hGSTA1-1 is much lower than that observed for the lipid-binding proteins, indicating a greater exposure of ANS to solvent when bound to hGSTA1-1. This is consistent with a solvent-exposed cleft at the dimer interface, the region to which ANS binds (see above).

The burial of hydrophobic surfaces of ANS and protein, and their desolvation during binding should result in favourable solvation entropy. However, the observed unfavourable entropy for wild-type hGSTA1-1 appears to contradict this. The entropic opposition to binding may be largely conformational in that binding may restrict the degrees of freedom of flexible or mobile groups on the interactive surfaces of ANS and protein. The conformational freedom of ANS can be described by two dihedral angles; the rotation about the N–C1′ bond between the anilino and naphthyl rings defining the angle between the plane of these rings, and the angle defined by C1′–N–C1–C2 ([44]; Figure 1). Unbound ANS is intrinsically flexible and its docking on to the protein would be penalized by conformational entropy.

We would like to thank Dr George Makhatadze for helpful comments and discussions on the manuscript. This work was supported by the University of the Witwatersrand, the Mellon Foundation, the South African National Research Foundation and the Wellcome Trust. Y.S. is the recipient of an African Explosives and Chemical Industries postgraduate scholarship.

REFERENCES

1 Coles, B. and Ketterer, B. (1990) The role of glutathione and glutathione transferases in chemical carcinogenesis. Crit. Rev. Biochem. Mol. Biol. **25**, 47–70
2 Waxman, D. J. (1990) Glutathione S-transferases: role in alkylating agent resistance and possible target for modulation chemotherapy – a review. Cancer Res. **50**, 6449–6454
3 Tsuchida, S. and Sato, K. (1992) Glutathione transferases and cancer. Crit. Rev. Biochem. Mol. Biol. **27**, 337–384
4 Hayes, J. D. and Pulford, D. J. (1995) The glutathione S-transferase supergene family: regulation of GST and the contribution of the isoenzymes to cancer chemoprotection and drug resistance. Crit. Rev. Biochem. Mol. Biol. **30**, 445–600
5 Listowsky, I. (1993) High capacity binding by glutathione S-transferases and glucocorticoid resistance. In Structure and Function of Glutathione Transferases (Tew, K. D., Pickett, C. B., Mantle, T. J., Mannervik, B. and Hayes, J. D., eds.), pp. 199–209, CRC Press, London
6 Armstrong, R. N. (1991) Glutathione S-transferases: reaction mechanism, structure, and function. Chem. Res. Toxicol. **4**, 131–140
7 Reinemer, P., Dirr, H. W., Ladenstein, R., Schaffer, J., Gallay, O. and Huber, R. (1991) The three-dimensional structure of class pi glutathione S-transferase in complex with glutathione sulfonate at 2.3 Å resolution. EMBO J. **10**, 1997–2005
8 Dirr, H., Reinemer, P. and Huber, R. (1994) Refined crystal structure of porcine class Pi glutathione S-transferase (pGST P1-1) at 2.1 Å resolution. J. Mol. Biol. **243**, 72–92
9 McTigue, M. A., Williams, D. R. and Tainer, J. A. (1995) Crystal structures of a schistosomal drug and vaccine target: glutathione S-transferase from *Schistosoma japonica* and its complex with the leading antischistosomal drug praziquantel. J. Mol. Biol. **246**, 21–27
10 Ji, X., von Rosenvinge, E. C., Johnson, W. W., Armstrong, R. N. and Gilliland, G. L. (1996) Location of a potential transport binding site in a sigma class glutathione transferase by x-ray crystallography. Proc. Natl. Acad. Sci. U.S.A. **93**, 8208–8213
11 Sluis-Cremer, N., Naidoo, N. N., Kaplan, W. H., Manoharan, T. H., Fahl, W. E. and Dirr, H. W. (1996) Determination of a binding site for a non-substrate ligand in mammalian cytosolic glutathione S-transferases by means of fluorescence-resonance energy transfer. Eur. J. Biochem. **241**, 484–488
12 Sluis-Cremer, N., Wallace, L., Burke, J., Stevens, J. and Dirr, H. (1998) Aflatoxin B1 and sulphobromophthalein binding to the dimeric human glutathione S-transferase A1-1: a fluorescence spectroscopic analysis. Eur. J. Biochem. **257**, 434–442
13 Vargo, M. A. and Colman, R. F. (2001) Affinity labelling of rat glutathione S-transferase isozyme 1-1 by 17β-iodoacetoxy-estradiol-3-sulfate. J. Biol. Chem. **276**, 2031–2036
14 Dirr, H. (2001) Folding and assembly of glutathione transferases. Chem. Biol. Interact. **133**, 19–23
15 Oakley, A. J., Lo, B. M., Nuccetelli, M., Mazzetti, A. P. and Parker, M. W. (1999) The ligandin (non-substrate) binding site of human Pi class glutathione transferase is located in the electrophile binding site (H-site). J. Mol. Biol. **291**, 913–926
16 Prade, L., Huber, R., Manoharan, T. H., Fahl, W. E. and Reuter, W. (1997) Structures of class pi glutathione S-transferase from human placenta in complex with substrate, transition-state analogue and inhibitor. Structure **5**, 1287–1295
17 Ji, X., Tordova, M., O'Donnell, R., Parsons, J. F., Hayden, J. B., Gilliland, G. L. and Zimniak, P. (1997) Structure and function of the xenobiotic substrate-binding site and location of a potential non-substrate-binding site in a class pi glutathione S-transferase. Biochemistry **36**, 9690–9702
18 Ji, X., Blaszczyk, J., Xiao, B., O'Donnell, R., Hu, X., Herzog, C., Singh, S. V. and Zimniak, P. (1997) Structure and function of residue 104 and water molecules in the xenobiotic substrate-binding site in human glutathione S-transferase P1-1. Biochemistry **38**, 10231–10238
19 Bhargava, M. M. and Dasgupta, A. (1988) Binding of sulfobromophthalein to rat and human ligandins: characterisation of a binding site peptide. Biochim. Biophys. Acta **955**, 296–300
20 Bico, P., Erhardt, J., Kaplan, W. and Dirr, H. (1995) Porcine class pi glutathione S-transferase: anionic ligand binding and conformational analysis. Biochim. Biophys. Acta. **1247**, 225–230
21 Boyer, T. D. (1986) Covalent labeling of the nonsubstrate ligand-binding site of glutathione S-transferases with bilirubin-Woodward's reagent K. J. Biol. Chem. **261**, 5363–5367
22 Nishihira, J., Ishibashi, T., Sakai, M., Nishi, S., Kondo, H. and Makita, A. (1992) Identification of the fatty acid binding site on glutathione S-transferase P. Biochem. Biophys. Res. Commun. **189**, 197–205
23 McCarthy, R. M., Farmer, P. and Sheehan, D. (1996) Binding of 2-hydroxy-5-nitrobenzyl alcohol to rat alpha class glutathione S-transferases; evidence for binding at tryptophan 21. Biochim. Biophys. Acta **1293**, 185–190

24 Bhargava, M. M., Ohmi, N., Listowsky, I. and Arias, I. M. (1980) Structural, catalytic, binding, and immunological properties associated with each of the two subunits of rat liver ligandin. J. Biol. Chem. **255**, 718–723
25 Bhargava, M. M., Ohmi, N., Listowsky, I. and Arias, I. M. (1980) Subunit composition, organic anion binding, catalytic and immunological properties of ligandin from rat testis. J. Biol. Chem. **255**, 724–727
26 Sinning, I., Kleywegt, G. J., Cowan, S. W., Reinemer, P., Dirr, H. W., Huber, R., Gilliland, G. L., Armstrong, R. N., Ji, X., Board, P. G. et al. (1993) Structure determination and refinement of human class alpha glutathione transferase A1-1, and a comparison with the Mu and Pi class enzymes. J. Mol. Biol. **232**, 192–212
27 Cameron, A. D., Sinning, I., L'Hermite, G., Olin, B., Board, P. G., Mannervik, B. and Jones, T. A. (1995) Structural analysis of human alpha-class glutathione transferase A1–1 in the apo-form and in complexes with ethacrynic acid and its glutathione conjugate. Structure **3**, 717–727
28 Dirr, H. W. and Wallace, L. A. (1999) Role of the C-terminal helix 9 in the stability and ligandin function of class alpha glutathione transferase A1-1. Biochemistry **38**, 15631–15640
29 Hornby, J. A., Luo, J. K., Stevens, J. M., Wallace, L. A., Kaplan, W., Armstrong, R. N. and Dirr, H. W. (2000) Equilibrium folding of dimeric class mu glutathione transferases involves a stable monomeric intermediate. Biochemistry **39**, 12336–12344
30 Stenberg, G., Bjornestedt, R. and Mannervik, B. (1992) Heterologous expression of recombinant human glutathione transferase A1-1 from a hepatoma cell line. Protein Expression Purif. **3**, 80–84
31 Laemmli, U. K. (1970) Cleavage of structural proteins during the assembly of the head of bacteriophage T4. Nature (London) **227**, 680–685
32 Habig, W. H. and Jakoby, W. B. (1981) Assays for differentiation of glutathione S-transferases. Methods Enzymol. **77**, 398–405
33 Lawrence, R. A. and Burk, R. F. (1976) Glutathione peroxidase activity in selenium-deficient rat liver. Biochem. Biophys. Res. Commun. **71**, 952–958
34 Wallace, L. A., Sluis-Cremer, N. and Dirr, H. W. (1998) Equilibrium and kinetic unfolding properties of dimeric human glutathione transferase A1-1. Biochemistry **37**, 5320–5328
35 Wallace, L. A., Blatch, G. L. and Dirr, H. W. (1998) A topologically conserved aliphatic residue in alpha-helix 6 stabilizes the hydrophobic core of domain II of glutathione transferases and is a structural determinant for the unfolding pathway. Biochem. J. **336**, 5320–5328
36 Lopez, M. M., Yutani, K. and Makhatadze, G. I. (1999) Interactions of the major cold shock protein of *Bacillus subtilis* CspB with single-stranded DNA templates of different base composition. J. Biol. Chem. **274**, 33601–33608
37 Brokx, R. D., Lopez, M. M., Vogel, H. J. and Makhatadze, G. I. (2001) Energetics of target peptide binding by calmodulin reveals different modes of binding. J. Biol. Chem. **276**, 14083–14091
38 Doyle, M. L. (1999) Titration calorimetry. In Current Protocols in Protein Science (Coligan, J. E., Dunn, B. M., Ploegh, H. L., Speicher, D. W. and Wingfield, P. T., eds.), pp. 20.4.1–20.4.24, John Wiley and Sons, New York
39 Fukada, H. and Takahashi, K. (1998) Enthalpy and heat capacity changes for the proton dissociation of various buffer components in 0.1 M potassium chloride. Proteins **33**, 159–166
40 Winder, A. F. and Gent, W. L. (1971) Correction of light-scattering errors in spectrophotometric protein determinations. Biopolymers **10**, 1243–1251
41 Sayed, Y., Wallace, L. A. and Dirr, H. W. (2000) The hydrophobic lock-and-key intersubunit motif of glutathione transferase A1-1: implications for catalysis, ligandin function and stability. FEBS Lett. **465**, 169–172
42 Wallace, L. A. and Dirr, H. W. (1999) Folding and assembly of dimeric human glutathione transferase A1-1. Biochemistry **38**, 16686–16694
43 Kirk, W. R., Kurian, E. and Prendergast, F. G. (1996) Characterization of the sources of protein-ligand affinity: 1-sulfonato-8-(1′)anilinonaphthalene binding to intestinal fatty acid binding protein. Biophys. J. **70**, 69–83
44 Ory, J. J. and Banaszak, L. J. (1999) Studies of the ligand binding reaction of adipocyte lipid binding protein using the fluorescent probe 1,8-anilinonaphthalene-8-sulfonate. Biophys. J. **77**, 1107–1116
45 Matulis, D. and Lovrien, R. (1998) 1-Anilino-8-naphthalene sulfonate anion-protein binding depends primarily on ion pair formation. Biophys. J. **74**, 422–429
46 Loladze, V. V., Ermolenko, D. N. and Makhatadze, G. I. (2001) Heat capacity changes upon burial of polar and nonpolar groups in proteins. Protein Sci. **10**, 1343–1352
47 Ladbury, J. E., Wright, J. G., Sturtevant, J. M. and Sigler, P. B. (1994) A thermodynamic study of the trp repressor-operator interaction. J. Mol. Biol. **238**, 669–681
48 Ladbury, J. E. (1995) Counting the calories to stay in the groove. Structure **3**, 635–639
49 Makhatadze, G. I. and Privalov, P. L. (1990) Heat capacity of proteins. I. Partial molar heat capacity of individual amino acid residues in aqueous solution: hydration effect. J. Mol. Biol. **213**, 375–384
50 Privalov, P. L. and Makhatadze, G. I. (1990) Heat capacity of proteins. II. Partial molar heat capacity of the unfolded polypeptide chain of proteins: protein unfolding effects. J. Mol. Biol. **213**, 385–391
51 Makhatadze, G. I. and Privalov, P. L. (1995) Energetics of protein structure. Adv. Protein Chem. **47**, 307–425
52 Stryer, L. (1965) The interaction of a naphthalene dye with apomyoglobin and apohemoglobin. A fluorescent probe of non-polar binding sites. J. Mol. Biol. **13**, 482–495
53 Weber, L. D., Tulinsky, A., Johnson, J. D. and El Bayoumi, M. A. (1979) Expression of functionality of alpha-chymotrypsin. The structure of a fluorescent probe-alpha-chymotrypsin complex and the nature of its pH dependence. Biochemistry **18**, 1297–1303

Received 29 November 2001; accepted 13 February 2002